
Feed-Forward Optimization With Delayed Feedback for Neural Networks

Katharina Flügel^{*,1,2} Daniel Coquelin^{1,2} Marie Weiel^{1,2}
 Charlotte Debus² Achim Streit² Markus Götz^{*,1,2}

¹Helmholtz AI

²Steinbuch Centre for Computing (SCC)
 Karlsruhe Institute of Technology (KIT)
 76344 Eggenstein-Leopoldshafen, Germany
 {firstname.lastname@kit.edu}

Abstract

Backpropagation has long been criticized for being biologically implausible, relying on concepts that are not viable in natural learning processes. This paper proposes an alternative approach to solve two core issues, i.e., weight transport and update locking, for biological plausibility and computational efficiency. We introduce **Feed-Forward with delayed Feedback (F³)**, which improves upon prior work by utilizing delayed error information as a sample-wise scaling factor to approximate gradients more accurately. We find that F³ reduces the gap in predictive performance between biologically plausible training algorithms and backpropagation by up to 96%. This demonstrates the applicability of biologically plausible training and opens up promising new avenues for low-energy training and parallelization.

1 Introduction

Today, nearly all artificial neural networks are trained with gradient-descent-based optimization methods [1]. Typically, backpropagation [2] is used to efficiently compute the network’s gradients. However, backpropagation relies on multiple biologically implausible factors, making it highly unlikely that the human brain functions in a similar fashion [3]. Besides increasing biological plausibility, solving these issues could significantly improve neural algorithms by increasing generalization performance, requiring fewer computational operations, and consuming less energy [4, 5]. As backpropagation makes up a significant portion of the computational and memory cost of neural network training, replacing it can yield significant time and energy savings. Diminishing the energy requirements is especially important in embedded and edge computing. Neuromorphic devices, for example, are novel brain-inspired hardware architectures [6] designed to accelerate neural networks and reduce the required energy. However, they are often unable to implement backpropagation and are thus in particular demand for biologically plausible alternatives [7].

Several training algorithms have been proposed to increase biological plausibility and reduce computational requirements. One option is removing the backward pass entirely, thus training an artificial neural network using only a forward pass. This can also lower the computational cost and open up new possibilities for parallelization but typically results in reduced predictive performance.

This paper presents **Feed-Forward with delayed Feedback (F³)**, our novel, biologically-inspired, backpropagation-free training algorithm for deep neural networks¹. F³ yields superior predictive performance on a variety of tasks compared to prior approaches by using delayed error information

¹Code available at github.com/Helmholtz-AI-Energy/f3

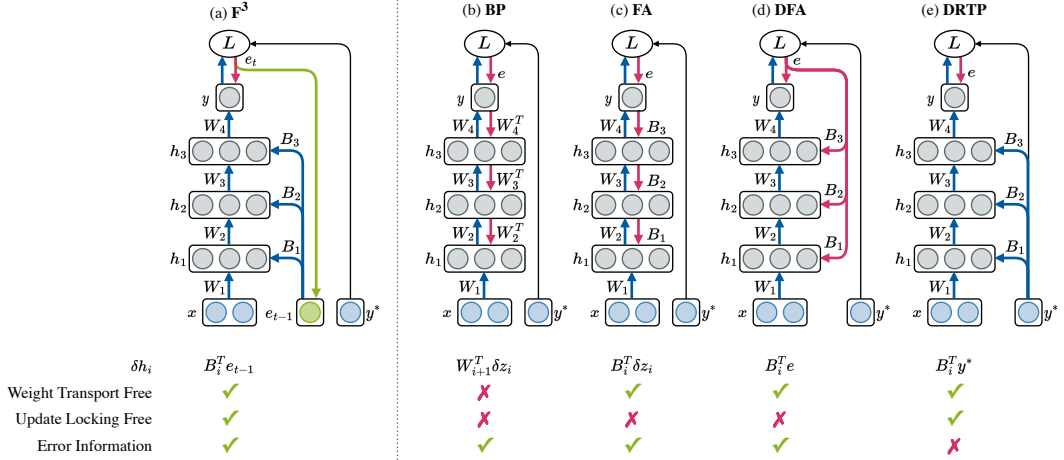


Figure 1: F^3 (a) solves both the weight transport and the update locking problem. In contrast to prior approaches, it uses delayed error information in the updates, improving the predictive performance. The current error signal e_t in epoch t is stored (green) and used in the forward pass (blue) of the next epoch $t + 1$. This eliminates the backward pass (red) for all hidden layers.

Previous approaches (b) to (e): Backpropagation (BP) (b) is not biologically plausible due to the weight transport and update locking problems caused by the backward pass. FA [8] (c) and DFA [9] (d) solve the weight transport problem by replacing the backward paths with random feedback weights B_i independent of the forward weights W_i . However, they are still update-locked as they depend on the current error e_t . DRTP [10] (e) releases update locking by using the target y^* instead of the error e_t , but this comes at the cost of reduced accuracy.

from previous epochs as feedback signals. Using fixed feedback weights, F^3 passes these feedback signals directly to each layer without layer-wise propagation. Together, this resolves the dependence on downstream layers, making it possible to update the network parameters during the forward pass. As a result, F^3 eliminates the need for the computationally expensive backward pass. This reduces both the computational cost and the required communication between layers, opening up promising possibilities for parallel and embedded training. F^3 also enables in-the-loop training on neuromorphic and edge devices, making it a promising candidate for application in low-powered computational settings.

Our main contributions are as follows:

- F^3 , a novel, biologically-inspired training algorithm for deep neural networks.
- Using delayed error information as feedback signal for improved predictive performance of backpropagation-free training.
- Empirical evaluation of F^3 on various datasets and neural network architectures.
- Theoretical analysis of the computational complexity of F^3 compared to backpropagation.

2 Related Work

While biological plausibility is not a necessary requirement for training artificial neural networks, there has been great interest in methods that combine biological plausibility with effective training [11, 5, 3, 12–14]. Two of the most substantial obstacles in that regard are the weight transport and the update locking problem [5, 10].

Weight Transport [15] Backpropagation reuses the forward weights symmetrically in the backward pass to propagate the gradients. However, synapses are unidirectional; and synchronizing separate forward and backward pathways precludes biological plausibility [16, 6]. The weights’ non-locality additionally constrains the memory access pattern, which can severely impact the computational efficiency [4].

Update Locking [17, 18] Artificial neural networks are typically trained with a clear separation between forward and backward passes. Every layer in a neural network must wait for all downstream layers to complete their forward and backward pass before completing its own backward pass. This introduces a considerable delay between a layer’s forward pass and the calculation of the gradients used to update its weights. This can significantly increase training times as results of the forward pass need to be buffered or recomputed [19, 10] and restricts parallelization. Moreover, it is not biologically plausible, as a neuron’s activation may have already changed during the delay, causing a desynchronization with the error signal [20].

Several approaches have been suggested to address both weight transport and update locking. Figure 1 illustrates some of these approaches compared to our approach F^3 .

To solve the weight transport problem, *target propagation* [13] replaces the loss gradients with layer-wise target values computed by auto-encoders. Using an additional linear correction, the so-called difference target propagation, this approach achieves results comparable to backpropagation. Ororbia and Mali [5] take a similar approach to target propagation but employ the current layer’s pre-activation and the next layer’s post-activation instead of generating the layer-wise targets with auto-encoders. *Feedback alignment (FA)* [8], illustrated in Figure 1 (c), replaces the forward weights with fixed random feedback weights in the backward pass, thereby demonstrating that symmetric feedback weights are not required for effective training. FA solves the weight transport problem; however, the training signals remain non-local, meaning the gradient estimates are propagated backward through the network’s hidden layers. To alleviate this, *direct feedback alignment (DFA)* [9] passes the error directly to each hidden layer, see Figure 1 (d).

For solving update locking, Mostafa et al. [19] use auxiliary classifiers to generate *local errors* from each layer’s output. With this strategy, they outperform FA and approach backpropagation-like accuracy. Improving upon this, Nøkland and Eidnes [21] demonstrate that combining local classifiers with a so-called local similarity matching loss can close the gap to backpropagation. *Decoupled greedy learning (DGL)* [22] follows a similar approach that is based on greedy objectives, which even scales to large datasets such as ImageNet [23].

Another approach to address update locking are *synthetic gradients* [18, 17], which model a subgraph of the network and predict its future output based on only local information. Replacing backpropagation with these synthetic gradients decouples the layers, resulting in so-called *decoupled neural interfaces (DNIs)*. The same approach can also be used to predict synthetic input signals and thus solve the *forward locking problem* [18]. *Direct random target projection (DRTP)* [10], illustrated in Figure 1 (e), builds upon DFA to solve weight transport and update locking simultaneously. By substituting the error with the targets, DFA’s direct backward paths can be replaced with direct forward paths to the hidden layers. While DRTP cannot reach the same accuracy as FA and DFA, it significantly outperforms training only the last layer of the network, demonstrating its ability to train hidden layers.

The *forward gradient* [24] is another approach to gradient approximation without backpropagation. It is based on forward mode automatic differentiation, which requires multiple runs to compute the exact gradient. To reduce this overhead, the gradient is estimated with the forward gradient based on the directional derivative.

The recently proposed *Forward-Forward (FF)* algorithm [25] replaces the backward pass with another forward pass on so-called negative data. Each layer is trained separately to distinguish the real data in the first forward pass from the negative data in the second forward pass. *PEPITA* [26] takes a similar approach by executing two forward passes on different input data, where the input to the second forward pass is modulated based on the error of the first one.

Multilayer SoftHebb [27] combines Hebbian learning with a softmax-based plasticity rule and a corresponding soft anti-Hebbian plasticity to enable training deep networks of a specific architecture. Using greedy layer-wise training, multilayer SoftHebb can train the hidden layers in a single unsupervised epoch, followed by up to 200 epochs of supervised training for the linear classifier head.

Predictive coding [28, 29] is another approach to biological plausibility based on the predicting processing model, an influential theory in cognitive neuroscience. It compares predictions of the expected input signal to a layer to the actual observations and aims to minimize this prediction error. In contrast to the more traditional feed-forward model, only the residual, the prediction error, is

passed to the next level [30]. Predictive coding has been successfully applied to artificial neural networks; for example, Whittington and Bogacz [31] show that predictive coding networks can approximate backpropagation on multilayer-perceptrons. This has since been extended to arbitrary computation graphs, including convolutional and recurrent neural networks [32].

3 Feed-Forward-Only Training

3.1 Training Neural Networks with Backpropagation

Let us consider a multi-layer fully-connected neural network like the one illustrated in Figure 1. It consists of K fully-connected layers where each layer i has weights W_i and biases b_i and passes its output h_i to the next layer. To obtain the network's output $y = h_K$, the forward pass computes the output of layer i as

$$z_i = W_i h_{i-1} + b_i \quad (1)$$

$$h_i = f(z_i), \quad (2)$$

with f being a non-linear activation function. A loss function L measures how close the last layer's output y is to the target value y^* . When training a neural network, we aim to decrease this loss by adjusting the network's parameters W_i and b_i . The *credit assignment problem* [33] states how much of the loss can be attributed to each parameter and how they should be changed accordingly. A common solution to the credit assignment problem is updating each parameter proportional to the gradient of the loss with respect to that parameter.

Backpropagation can compute this gradient efficiently by applying the chain rule in a backward pass over the network. For example, it computes the gradient of the loss with respect to h_i as

$$\delta h_i = \frac{\partial L}{\partial h_i} = W_{i+1}^T \delta z_{i+1}, \quad (3)$$

which can also be expressed as

$$\delta h_i = W_{i+1}^T (\delta h_{i+1} \odot f'(z_{i+1})) \quad (4)$$

$$= \boxed{\frac{\partial L}{\partial y}} \boxed{W_{i+1}^T \left(\frac{\partial y}{\partial h_{i+1}} \odot f'(z_{i+1}) \right)}. \quad (5)$$

The gradient δh_i thus depends on an error term (green), represented by $\partial L / \partial y$, and the feedback path (blue). This feedback path relies on both the transpose of the forward weights W_j^T and the derivative of the activation f at the input z_j for all downstream layers $j \in \{i+1, \dots, K\}$. The gradients of the weights W_i and biases b_i can be derived directly from δh_i .

3.2 Approximating Gradients without Backpropagation

Not all of the information necessary to compute δh_i as described in Equation (5) is available to a biologically plausible training algorithm, as a) the algorithm cannot rely on symmetric feedback weights (weight transport) and thus cannot utilize the forward weights W or their transpose, and b) the update step cannot wait for the downstream layers $j > i$ (update locking). Thus, neither the intermediate values z_j , the final output y , nor the loss L is available. This means that biologically plausible training algorithms cannot compute the true gradient δh_i . Instead, they typically approximate the gradients based on the information that is available.

F^3 is inspired by DRTP [10], which approximates the gradients δh_i using the targets y^* instead of the error signal and fixed random feedback weights for the feedback path. However, the targets are not a practically good approximation of the true error signal as they contain no information on the error magnitude and only limited information on its direction, which can severely impact the training. Therefore, we propose *Feed-Forward with delayed Feedback* (F^3), which uses delayed error information e_{t-1} to approximate the error signal more precisely while remaining update locking free.

Algorithm 1 Training a fully-connected neural network M with K layers for t_{\max} epochs using F^3 .

Input: model M , optimizer Opt , data x, y^* , epochs t_{\max}

$$e_0 \leftarrow y^*$$

for $t \leftarrow 1$ **to** t_{\max} **do**

$$h_0 \leftarrow x$$

for $i \leftarrow 1$ **to** K **do**

$$h_i \leftarrow f(W_i h_{i-1} + b_i)$$

if $i \neq K$ **then**

$$\delta^{F^3} h_i \leftarrow B_i^T e_{t-1}$$

else

$$\delta^{F^3} h_K \leftarrow \frac{\partial L(h_K, y^*)}{\partial h_K}$$

end if

$$\delta^{F^3} z_i \leftarrow \delta^{F^3} h_i \odot f'(z_i)$$

$$\delta^{F^3} W_i \leftarrow \delta^{F^3} z_i h_{i-1}^T$$

$$\delta^{F^3} b_i \leftarrow \delta^{F^3} z_i$$

$$W_i, b_i \leftarrow Opt.update_weights(\delta^{F^3} W_i, \delta^{F^3} b_i)$$

end for

$$e_t \leftarrow \text{error_information}(h_K, y^*)$$

end for

3.3 Delayed Error Information as Feedback Signal

F^3 , illustrated in Figure 1 (a), approximates the gradient δh_i as

$$\delta^{F^3} h_i = \boxed{B_i^T} \boxed{e_{t-1}}. \quad (6)$$

We reuse the idea of fixed feedback weights B_i to replace the feedback path (blue) but use delayed error information e_{t-1} as error signal (green). Computing $\delta^{F^3} h_i$ is thus independent of other layers. The remaining gradients within the layer, e.g., for the weights and biases, rely only on the incoming gradient δh_i and information within the layer itself. They can be computed with the chain rule in the same way as with backpropagation using the approximate gradient $\delta^{F^3} h_i$. This makes all gradient approximations independent of downstream layers and allows updating a layer immediately during the forward pass, eliminating the need for a separate backward pass. Since the final layer K has access to the model's output $y = y_K$, it can use the current error signal and compute the true gradients. As a result, F^3 only affects hidden layers; the output layer is updated as it would be with backpropagation.

Algorithm 1 outlines how F^3 is used to train a fully-connected neural network. The layers are processed in a forward pass which computes the layer's output h_i , followed immediately by computing the approximate gradients $\delta^{F^3} W_i$ and $\delta^{F^3} b_i$ and updating the layer's parameters W_i and b_i . The approximate gradients can be used to update the network's parameters like the true gradients. For example, using stochastic gradient descent with a learning rate of η would result in the update

$$W_i \leftarrow W_i - \eta \delta^{F^3} W_i \quad (7)$$

$$b_i \leftarrow b_i - \eta \delta^{F^3} b_i. \quad (8)$$

F^3 is thus independent of the optimizer and can be used with various gradient-based optimizers from standard SGD to more advanced methods like Adam [34].

F^3 utilizes sample-wise delayed error information

$$e_{t-1} = \left(\frac{\partial L}{\partial y} \right)_{t-1} \quad (9)$$

from the previous epoch $t - 1$ to approximate the current error signal

$$e_t = \left(\frac{\partial L}{\partial y} \right)_t. \quad (10)$$

The feedback is thus always delayed by one epoch. The targets y^* are used to initialize the error information in the first epoch. Alternatively, the error information can be initialized from an additional inference-only epoch $t = 0$, leaving the model parameters unchanged. On a technical level, F^3 stores each training sample’s error information at the end of the forward pass. As the loss is already used to train the last layer, this requires no additional computation.

Delayed error information more closely resembles the actual error signal than, for example, the targets y^* used in prior, similarly plausible approaches [10]. Using delayed error information includes both the magnitude and direction of the error in the update, which helps to differentiate between samples requiring more attention and those not. F^3 thus offers a more accurate gradient approximation.

3.4 Different Variants of Delayed Error Information

The sample-wise gradient of the loss with respect to the model’s output y_{t-1} is the most natural choice for modeling the error signal as it corresponds to the information used in backpropagation delayed by one epoch. However, F^3 can also use other types of delayed error information. For example, it can use the delayed error

$$y^* - y_{t-1}. \quad (11)$$

We refer to these two variants as F^3 -Loss and F^3 -Error.

Additional transformations can be applied to the chosen error information. For classification tasks, one could consider only the feedback signal of the target class c^* . We refer to this as *one-hot error information* as it corresponds to multiplying the error information with the one-hot encoded targets. One-hot error information reduces the computational cost of the gradient approximation by reducing the matrix-vector multiplication $B_i^T e_{t-1}$ to the multiplication of a single column of B_i with the scalar $e_{t-1}[c^*]$. Another option is applying an additional softmax to the output y_{t-1} before computing the error information.

Instead of sample-wise error information, one could also aggregate the error over all samples in the last epoch. This would reduce the already small memory overhead to just a single value for the whole training set, which could benefit applications with severe hardware constraints. While losing the ability to differentiate between low and high error samples, this still adjusts the update step size as the error decreases throughout the training.

3.5 How F^3 Solves the Weight Transport Problem

Prior work [8–10] has shown that neural networks can be trained using fixed random feedback paths. We therefore replace the layer-wise propagation of gradients (blue) in Equation (5) with a fixed feedback weight matrix B_i to directly pass the error signal to layer i in Equation (6). All gradient information other than the error signal, e.g., the forward weights and the derivatives of the activation functions for all downstream layers, is encoded in this feedback weight matrix. The forward weights W_j are thus no longer required to approximate the gradient $\delta^{F^3} h_i$, making F^3 defacto weight transport free.

3.6 How F^3 Solves the Update Locking Problem

As discussed in Section 3.2, avoiding update locking means that the update step in layer i cannot rely on results or gradients in downstream layers $j > i$. Using fixed direct feedback paths already eliminates the dependence on downstream layers in the feedback path. The error signal $\partial L / \partial y$ (green) in Equation (5) is not available either, as the last layer’s output y has not yet been computed for the current epoch t . Since training typically requires multiple epochs, F^3 instead uses delayed error information from the previous epoch $t - 1$ to approximate the current error signal in Equation (6). As discussed in Section 3.3, this makes it independent of downstream layers.

This introduces a dependency between consecutive epochs, as processing a sample requires its delayed error information from the previous epoch. However, this is generally not a problem since training epochs are typically clearly separated. Often, there is even additional auxiliary computation in between epochs, such as intermediate evaluation or check-pointing. One could also relax this requirement at the cost of a potentially higher delay of the error information by using the most

current loss available for a sample, be it from the previous or any earlier epoch. In summary, F^3 can immediately update the weights in every layer without waiting for downstream layers and is thus free of update locking.

3.7 Computational Considerations

By eliminating layer-wise error propagation, F^3 generally requires fewer operations than backpropagation. The exact reduction depends on the input data and selected network architecture. For a fully-connected neural network with K linear layers of equal width w , input size n_0 , and output size C , the number of fused multiply-add operations to perform the forward, backward, and update step for a single training sample is

$$3w(n_0 + (K-2)w + C) + \underbrace{(K-2)w^2 + Cw}_{\text{computing } \delta y_i} \quad (12)$$

with backpropagation and

$$3w(n_0 + (K-2)w + C) + \underbrace{C(K-1)w}_{\text{computing } \delta^{F^3} y_i}. \quad (13)$$

with F^3 . The detailed derivation of these equations is given in Appendix A. The number of operations saved increases with deeper and wider networks. For sufficiently large widths, F^3 approaches a 100% reduction for computing the δy_i . This results in a 25% theoretical maximum reduction in time for the whole training step, i.e., forward and backward pass followed by an update step.

As an example, we consider a five layer network with input size $n_0 = 100$ and output size $C = 10$. With a hidden layer width $w = 200$, F^3 can save more than 90% of operations computing the δy_i and more than 20% in total throughout the whole batch. With a width of $w = 1024$, this increases to more than 98% and 24%, respectively. In experimental evaluations, we find that the practically achievable reduction in training time is closer to 15%.

4 Evaluation

4.1 Methods

We evaluate F^3 on different datasets and learning tasks. For image classification, we use the well-known image classification datasets MNIST [35] and CIFAR-10 [36]. For general classification, we use the Census Income dataset [37] to predict whether a person's income exceeds a threshold based on their census data. For regression, we use the SGEMM dataset [38, 39] to predict the run time of sparse matrix-matrix multiplications on GPU using different kernel parameters. The MNIST, CIFAR-10, and SGEMM datasets have been standardized.

We use F^3 to train different fully-connected neural network architectures with 1 to 50 hidden layers at a width of 500 neurons. We use the hyperbolic tangent activation function in hidden layers and a sigmoid in the output layer for classification tasks. For classification tasks, one-hot encoding with binary cross-entropy (BCE) loss is used, while mean squared error (MSE) loss is used for regression tasks. We set a fixed learning rate determined by a grid search, as shown in Tables 2 and 3, and use the Adam optimizer [34] with default parameters.

We compare multiple variants of F^3 using the different options for delayed error information described in Section 3.4. Results are shown for both the delayed loss gradient and the delayed error as feedback signal. Unless otherwise mentioned, we use the one-hot error information for classification tasks, i.e., using only the feedback coming from the target class. For regression tasks, we always use the delayed feedback signal directly without further modifications.

We compare F^3 to multiple other training algorithms: backpropagation and DRTP [10] were chosen as baselines for traditional and biologically plausible training approaches, respectively. To demonstrate the benefits of biologically plausible approaches, we include the results of training only the last layer while keeping the hidden layers constant at their random initialization. We refer to this as last-layer-only (LLO) training in the following. We additionally include DFA [9], which corresponds to F^3 using current instead of delayed error information, thus not solving update locking.

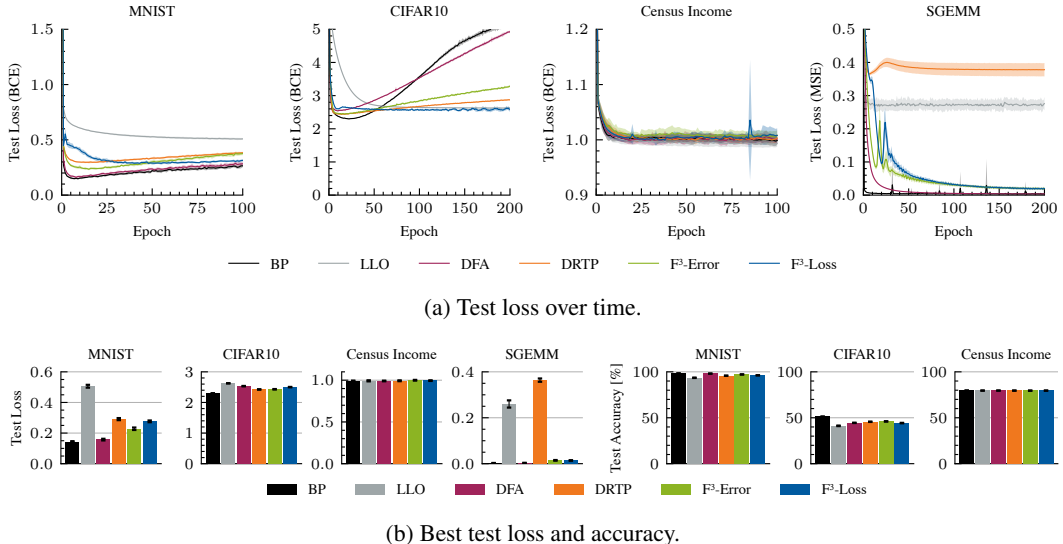


Figure 2: Test loss and accuracy using different training approaches for a fully-connected neural network with one hidden layer consisting of 500 neurons. We evaluate two variants of F^3 , using either the error or the loss gradient as delayed error information, and compare them to backpropagation, last-layer-only (LLO) training, DFA, and DRTP on the classification tasks MNIST, CIFAR-10, Census Income, and the regression task SGEMM. By using delayed error information as feedback signal, F^3 improves upon the performance of the similarly plausible DRTP, thus closing the gap of update locking free training to backpropagation.

4.2 Experimental Environment

All experiments were conducted on a single compute node with two Intel Xeon 8386 “Ice Lake” processors and four NVIDIA A100-40 tensor core GPUs. Models were implemented in Python 3.8.6 using the PyTorch framework [40] version 1.12.1 with CUDA version 11.6. The source code is publicly available at github.com/Helmholtz-AI-Energy/f3.

4.3 Delayed Error Information

Figure 3 illustrates the performance of F^3 using the different variants of delayed error information introduced in Section 3.4. For classification, error-based updates (F^3 -Error, green) tend to outperform updates based on the gradient of the loss (F^3 -Loss, blue). This result is unexpected since F^3 -Loss is more similar to backpropagation than F^3 -Error from a theoretical point of view. When using MSE loss, e.g., for the regression task SGEMM, the error is equivalent to the loss gradient except for a scalar factor. In this case, the utilized error information affects only the step size but not the general direction of the update step. Both effects can also be observed in Figure 2.

For classification, we test additional transformations of the error information, applying either a softmax to the output or considering only the error information of the target class, which corresponds to multiplication with the one-hot encoded target. In Figure 3, these variants are highlighted with different markers. We find that both the raw error information and the one-hot version are valid options for effective training, whereas applying an additional softmax tends to decrease the resulting quality as measured by an increased test loss.

4.4 Comparison to Other Training Algorithms

Figure 2 illustrates the behavior of different training algorithms for multiple datasets and tasks. The exact results are also given in Tables 4 and 5. As expected, backpropagation outperforms biologically plausible training on most datasets; however, F^3 reduces this gap in performance by a significant fraction. On MNIST, F^3 -Error noticeably outperforms DRTP, increasing the test accuracy from 95.8% to 97.2%, thus reducing the gap to backpropagation by 54.9%. None of the algorithms

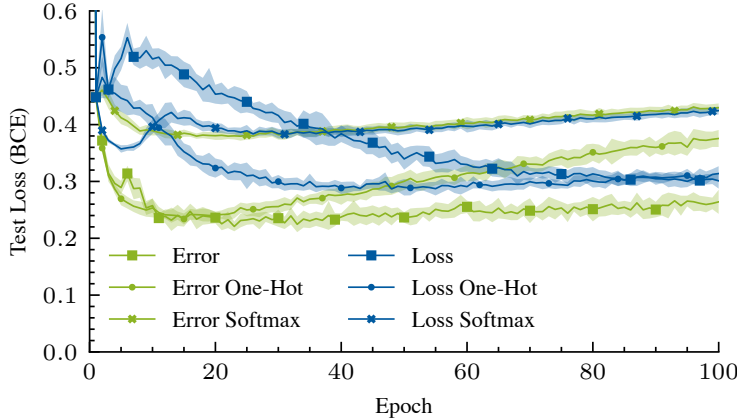


Figure 3: Test loss for F^3 using different types of delayed error information when training a fully-connected neural network with one hidden layer consisting of 500 neurons each on MNIST. The error tends to give better training results than the gradient of the loss. The one-hot transformed error signal provides similar results to the raw error information, whereas softmax offers no advantage but rather increases the resulting test loss.

solve the CIFAR-10 image classification task to an acceptable level, with even backpropagation only reaching a test accuracy of 51.2%. This is likely due to a sub-optimal network architecture. Counterintuitively, F^3 and DRTP slightly outperform DFA on CIFAR-10. Comparing to Frenkel et al. [10]’s results, we suspect this is caused by DFA requiring a significantly lower learning rate for CIFAR-10 than other biologically plausible approaches and might thus require a more fine-grained hyper-parameter optimization differentiating more between the different algorithms.

All tested algorithms achieve good performance of about 80% on the Census Income dataset within less than ten epochs. On the regression dataset SGEMM, F^3 reduces the test loss from 0.364 to 0.014, thus reducing the gap to backpropagation by 96.9%. F^3 performs significantly better than LLO on all datasets except Census Income, where the difference between all methods is minor. This demonstrates the effectiveness of the biologically plausible update rule for hidden layers, proving that F^3 is more than just a sophisticated scheme to train the output layer.

In summary, F^3 notably improves upon the similarly plausible DRTP for both MNIST and the SGEMM regression task. On CIFAR-10, none of the algorithms shown solved the task to a satisfying level for the tested network architecture. All algorithms solved the Census Income classification problem to a similar degree, indicating that current biologically plausible algorithms are already applicable to some tasks without significant performance declines compared to backpropagation.

4.5 Impact of the Feedback Weight Initialization

We further explore different approaches to initializing the feedback weights B_i and their impact on the training. As a baseline, we use the Kaiming-He uniform distribution [41] with a gain of $\sqrt{2}$ and the fan-in mode. To test the impact of the feedback weights’ magnitude and sign, we consider two discrete uniform distributions: trinomial with the values $\{-1, 0, 1\}$ and binomial with the values $\{0, 1\}$. Finally, we test repeating the identity matrix I along the larger dimension with alternating signs, referred to as $\pm I$. Figure 4 illustrates these initialization methods. Note that the bounds of the Kaiming-He distribution can become very small for large matrices.

Figure 5 shows the test loss for the different initialization methods for DRTP and F^3 -Error. With both training algorithms, we observe a small but notable improvement using trinomial initialization over Kaiming uniform, indicating that continuous magnitudes are not necessary for effective learning. In contrast to trinomial initialization, binomial initialization results in a massive increase in loss. This is a clear indication that the sign of the values plays a significant role and is necessary for successfully communicating the feedback signals. Repeating the identity matrix is similarly in-

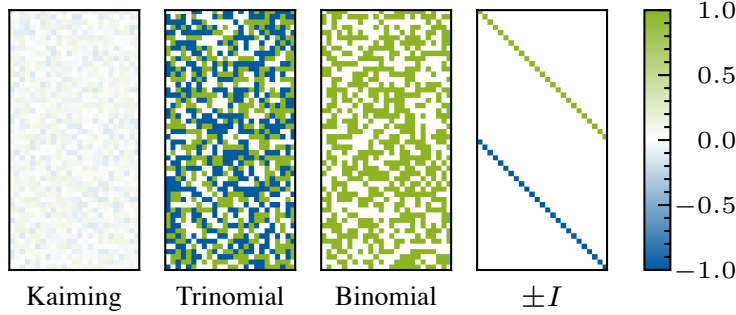


Figure 4: The different feedback weight initialization schemes. Kaiming uses the Kaiming-He uniform distribution with a gain of $\sqrt{2}$ and the fan-in mode. Trinomial and binomial are discrete uniform distributions over the values $\{-1, 0, 1\}$ and $\{0, 1\}$, respectively. $\pm I$ repeats the identity matrix I along the larger dimension, alternating the sign.

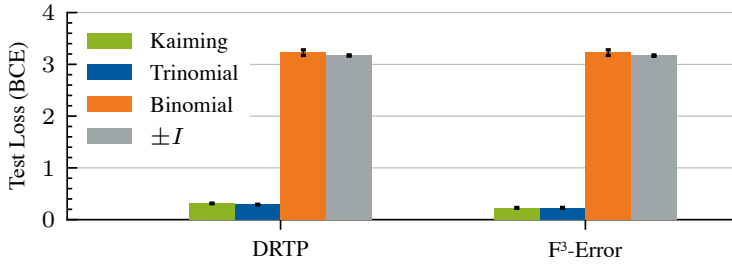


Figure 5: Best test loss for DRTP and F^3 with error scaling using different feedback weight initialization methods, shown for a fully-connected neural network with one hidden layer of 500 neurons trained on MNIST for 100 epochs. Trinomial initialization offers a slight improvement over the baseline Kaiming initialization, while neither binomial nor $\pm I$ allow effective training.

effective, suggesting that the arrangement of feedback weights matters even with both positive and negative values.

These results illustrate that feed-forward training algorithms do not depend on a specific initialization of the feedback weights, but certain characteristics are necessary to promote effective training. Namely, they require a combination of different signs in the rows of the two-dimensional feedback weight matrix. The feedback weights B_i of layer i are used to approximate the gradient δh_i according to Equation (6). Each column in the matrix B_i is used to compute one value in $\delta^F h_i$ via a dot product with the feedback signal e_{t-1} . The feedback signal consists of one value per model output, e.g., one value per class. For classification, a column in B_i thus prescribes the class mixture of the feedback for each value in $\delta^F h_i$. Only columns with more than one non-zero value allow multi-class mixtures, explaining the ineffectiveness of $\pm I$. Furthermore, different signs help separate classes from each other, as shown by the improved performance of trinomial over binomial initialization.

4.6 Scaling with Network Depth

Figure 6 shows the scaling behavior of the different training approaches with increasing network depth. Biologically plausible algorithms appear more robust to problems typically arising with very deep networks. While training smaller networks very effectively, we find that backpropagation fails to train networks with more than 25 layers, offering virtually no improvement over random initialization. In contrast, F^3 can train shallow networks to nearly the same degree of predictive performance as backpropagation while diminishing considerably less sharply with increasing depth. This is a result of the direct feedback pathways [9], which are independent of the network’s depth and thus immune to the typical problems arising when training very deep networks with backprop-

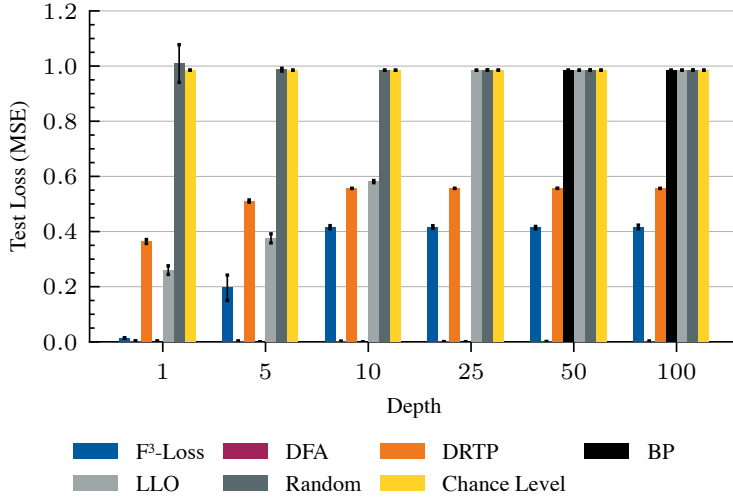


Figure 6: Test loss on the SGEMM dataset for different network depths and a width of 500 neurons per layer. Feed-forward-only training algorithms like F^3 , DFA, and DRTP are more robust to very deep networks, while backpropagation fails to train networks above a depth of 25, achieving no improvement over the random initialization.

agation [42]. This immunity is highlighted by DFA, which is unaffected by the network depth as expected from Nøkland [9]’s results.

The scaling behavior for DRTP is similar to F^3 , i.e., the performance decreases much more slowly with network depth than when training with backpropagation. As both DRTP and F^3 are based on direct random feedback pathways, this result was expected. However, DRTP performs much worse for regression problems and cannot train even more shallow networks on the SGEMM task to a similar predictive performance as F^3 . In summary, both biologically plausible algorithms can train even deep, 100-layer networks without further remedies, such as specific activation functions, yet F^3 offers better predictive performance throughout all tested network depths.

5 Conclusion

Backpropagation relies on concepts infeasible in natural learning, rendering it an effective yet biologically implausible and computationally expensive approach to training artificial neural networks. In this paper, we introduce Feed-Forward with delayed Feedback (F^3), a novel algorithm for backpropagation-free training of multi-layer neural networks using a feed-forward approximation of intermediate gradients based on delayed error information. F^3 solves the weight transport problem by implementing direct random feedback connections and avoids update locking by using the delayed error information from the previous epoch as an additional sample-wise scaling factor. This makes it more biologically plausible than backpropagation while reducing training time and energy consumption per epoch. F^3 significantly improves the predictive performance compared to previous update locking free algorithms, reducing the gap to backpropagation by over 50% for classification and more than 95% for regression tasks.

By addressing the weight transport and update locking problems, F^3 is more biologically plausible than backpropagation. However, some implausibilities remain, such as the spiking problem, Dale’s Law, and the general implausibility of supervised learning [3, 43]. A further limitation is the remaining accuracy gap to backpropagation and F^3 frequently requiring more epochs to reach a similar accuracy. This also limits the applicability to large-scale tasks and often outweighs the benefit of reduced compute requirements per epoch. Furthermore, there is currently no natural way to apply F^3 to convolutional networks while retaining the advantages of weight sharing for the feedback weights. The most promising next steps for more biological plausibility are combining F^3 with approaches like spiking neural networks [44] and semi- or self-supervised learning. To increase the

predictive performance, improving the feedback pathways and applying F^3 more effectively to other architectures are essential to scale F^3 to larger tasks.

By releasing update locking and thus the inter-layer dependencies when computing the gradients, F^3 can update the network's parameters during the forward pass. As a result, F^3 eliminates the need for the computationally expensive backward pass, thus requiring fewer operations and removing the need to buffer or recompute activations. Beyond that, it opens up promising possibilities for parallel training setups like pipeline parallelism by reducing the amount of communication and synchronization between different layers. Furthermore, F^3 enables on-device training on highly promising neuromorphic devices, which would simplify the training process significantly and has the potential to economize compute resources and energy tremendously.

Acknowledgments and Disclosure of Funding

This work is supported by the Helmholtz Association Initiative and Networking Fund under the Helmholtz AI platform and the HAICORE@KIT grant.

References

- [1] I. Goodfellow, Y. Bengio, and A. Courville, *Deep Learning*. MIT Press, 2016.
- [2] D. E. Rumelhart, G. E. Hinton, and R. J. Williams, “Learning representations by back-propagating errors,” *Nature*, vol. 323, no. 6088, pp. 533–536, Oct. 1986, number: 6088 Publisher: Nature Publishing Group.
- [3] Y. Bengio, D.-H. Lee, J. Bornschein, T. Mesnard, and Z. Lin, “Towards biologically plausible deep learning,” 2016, arXiv:2202.08587.
- [4] B. Crafton, M. West, P. Basnet, E. Vogel, and A. Raychowdhury, “Local learning in RRAM neural networks with sparse direct feedback alignment,” in *IEEE/ACM International Symposium on Low Power Electronics and Design*, Jul. 2019, pp. 1–6.
- [5] A. G. Ororbia and A. Mali, “Biologically motivated algorithms for propagating local target representations,” *Proceedings of the AAAI Conference on Artificial Intelligence*, vol. 33, no. 1, pp. 4651–4658, Jul. 2019.
- [6] J. Tang, F. Yuan, X. Shen, Z. Wang, M. Rao, Y. He, Y. Sun, X. Li, W. Zhang, Y. Li, B. Gao, H. Qian, G. Bi, S. Song, J. J. Yang, and H. Wu, “Bridging biological and artificial neural networks with emerging neuromorphic devices: Fundamentals, progress, and challenges,” *Advanced Materials*, vol. 31, no. 49, p. 1902761, 2019.
- [7] C. Frenkel, J.-D. Legat, and D. Bol, “A 28-nm convolutional neuromorphic processor enabling online learning with spike-based retinas,” in *IEEE International Symposium on Circuits and Systems*, Oct. 2020, pp. 1–5, iSSN: 2158-1525.
- [8] T. P. Lillicrap, D. Cownden, D. B. Tweed, and C. J. Akerman, “Random synaptic feedback weights support error backpropagation for deep learning,” *Nature Communications*, vol. 7, no. 1, p. 13276, Nov. 2016.
- [9] A. Nøkland, “Direct feedback alignment provides learning in deep neural networks,” in *Proceedings of the 30th International Conference on Neural Information Processing Systems*, ser. NIPS’16. Red Hook, NY, USA: Curran Associates Inc., Dec. 2016, pp. 1045–1053.
- [10] C. Frenkel, M. Lefebvre, and D. Bol, “Learning without feedback: Fixed random learning signals allow for feedforward training of deep neural networks,” *Frontiers in Neuroscience*, vol. 15, 2 2021.
- [11] J. C. R. Whittington and R. Bogacz, “Theories of error back-propagation in the brain,” *Trends in Cognitive Sciences*, vol. 23, no. 3, pp. 235–250, Mar. 2019.
- [12] A. Tavanaei, M. Ghodrati, S. R. Kheradpisheh, T. Masquelier, and A. Maida, “Deep learning in spiking neural networks,” *Neural Networks*, vol. 111, pp. 47–63, Mar. 2019.

- [13] D.-H. Lee, S. Zhang, A. Fischer, and Y. Bengio, “Difference target propagation,” in *Machine Learning and Knowledge Discovery in Databases*, ser. Lecture Notes in Computer Science, A. Appice, P. P. Rodrigues, V. Santos Costa, C. Soares, J. Gama, and A. Jorge, Eds. Cham: Springer International Publishing, 2015, pp. 498–515.
- [14] Q. Liao, J. Leibo, and T. Poggio, “How important is weight symmetry in backpropagation?” in *Proceedings of the Thirtieth AAAI Conference on Artificial Intelligence*, vol. 30, Feb. 2016, pp. 1837–1844.
- [15] S. Grossberg, “Competitive learning: From interactive activation to adaptive resonance,” *Cognitive Science*, vol. 11, no. 1, pp. 23–63, Jan. 1987.
- [16] S. Zeki, “A massively asynchronous, parallel brain,” *Philosophical Transactions of the Royal Society B: Biological Sciences*, May 2015.
- [17] W. M. Czarnecki, G. Świrszcz, M. Jaderberg, S. Osindero, O. Vinyals, and K. Kavukcuoglu, “Understanding synthetic gradients and decoupled neural interfaces,” in *Proceedings of the 34th International Conference on Machine Learning*. PMLR, Jul. 2017, pp. 904–912, iSSN: 2640-3498.
- [18] M. Jaderberg, W. M. Czarnecki, S. Osindero, O. Vinyals, A. Graves, D. Silver, and K. Kavukcuoglu, “Decoupled neural interfaces using synthetic gradients,” in *Proceedings of the 34th International Conference on Machine Learning*. PMLR, Jul. 2017, pp. 1627–1635, iSSN: 2640-3498.
- [19] H. Mostafa, V. Ramesh, and G. Cauwenberghs, “Deep supervised learning using local errors,” *Frontiers in Neuroscience*, vol. 12, p. 608, 2018.
- [20] E. Hunsberger, “Spiking deep neural networks: Engineered and biological approaches to object recognition,” Ph.D. dissertation, University of Waterloo, 2018.
- [21] A. Nøkland and L. H. Eidnes, “Training neural networks with local error signals,” in *Proceedings of the 36th International Conference on Machine Learning*. PMLR, May 2019, pp. 4839–4850.
- [22] E. Belilovsky, M. Eickenberg, and E. Oyallon, “Decoupled greedy learning of cnns,” in *Proceedings of the 37th International Conference on Machine Learning*. PMLR, Nov. 2020, pp. 736–745, iSSN: 2640-3498.
- [23] J. Deng, W. Dong, R. Socher, L.-J. Li, K. Li, and L. Fei-Fei, “ImageNet: A large-scale hierarchical image database,” in *IEEE Conference on Computer Vision and Pattern Recognition*, Jun. 2009, pp. 248–255, iSSN: 1063-6919.
- [24] A. G. Baydin, B. A. Pearlmutter, D. Syme, F. Wood, and P. Torr, “Gradients without backpropagation,” Feb. 2022, arXiv:2202.08587.
- [25] G. Hinton, “The forward-forward algorithm: Some preliminary investigations,” 2022, arXiv:2212.13345.
- [26] G. Dellafererra and G. Kreiman, “Error-driven Input Modulation: Solving the Credit Assignment Problem without a Backward Pass,” Jul. 2022, arXiv:2201.11665.
- [27] A. Journé, H. G. Rodriguez, Q. Guo, and T. Moraitis, “Hebbian deep learning without feedback,” Sep. 2022, arXiv:2209.11883.
- [28] K. Friston, “A theory of cortical responses,” *Philosophical Transactions of the Royal Society B: Biological Sciences*, vol. 360, no. 1456, pp. 815–836, 2005.
- [29] R. P. N. Rao and D. H. Ballard, “Predictive coding in the visual cortex: a functional interpretation of some extra-classical receptive-field effects,” *Nature Neuroscience*, vol. 2, no. 1, pp. 79–87, 1999.
- [30] K. S. Walsh, D. P. McGovern, A. Clark, and R. G. O’Connell, “Evaluating the neurophysiological evidence for predictive processing as a model of perception,” *Annals of the New York Academy of Sciences*, vol. 1464, no. 1, pp. 242–268, 2020.

- [31] J. C. R. Whittington and R. Bogacz, “An approximation of the error backpropagation algorithm in a predictive coding network with local hebbian synaptic plasticity,” *Neural Computation*, vol. 29, no. 5, pp. 1229–1262, 2017.
- [32] B. Millidge, A. Tschantz, and C. L. Buckley, “Predictive coding approximates backprop along arbitrary computation graphs,” *Neural Computation*, vol. 34, no. 6, pp. 1329–1368, 2022.
- [33] M. Minsky, “Steps toward Artificial Intelligence,” *Proceedings of the IRE*, vol. 49, no. 1, pp. 8–30, Jan. 1961.
- [34] D. P. Kingma and J. Ba, “Adam: A method for stochastic optimization,” in *3rd International Conference on Learning Representations*, Y. Bengio and Y. LeCun, Eds. ICLR, 2015.
- [35] Y. LeCun, L. Bottou, Y. Bengio, and P. Haffner, “Gradient-based learning applied to document recognition,” *Proceedings of the IEEE*, vol. 86, no. 11, pp. 2278–2324, 1998.
- [36] A. Krizhevsky, “Learning multiple layers of features from tiny images,” University of Toronto, Tech. Rep., 2009.
- [37] R. Kohavi, “Scaling up the accuracy of naive-bayes classifiers: A decision-tree hybrid,” in *KDD’96: Proceedings of the Second International Conference on Knowledge Discovery and Data Mining*. AAAI Press, Dec. 1996, pp. 202–207.
- [38] C. Nugteren and V. Codreanu, “CLTune: A generic auto-tuner for OpenCL kernels,” in *2015 IEEE 9th International Symposium on Embedded Multicore/Many-core Systems-on-Chip*, 2015, pp. 195–202.
- [39] R. Ballester-Ripoll, E. G. Paredes, and R. Pajarola, “Sobol tensor trains for global sensitivity analysis,” 2017, arXiv:1712.00233.
- [40] A. Paszke, S. Gross, F. Massa, A. Lerer, J. Bradbury, G. Chanan, T. Killeen, Z. Lin, N. Gimelshein, L. Antiga, A. Desmaison, A. Kopf, E. Yang, Z. DeVito, M. Raison, A. Tejani, S. Chilamkurthy, B. Steiner, L. Fang, J. Bai, and S. Chintala, “Pytorch: An imperative style, high-performance deep learning library,” in *Advances in Neural Information Processing Systems*, vol. 32. Curran Associates, Inc., 2019.
- [41] K. He, X. Zhang, S. Ren, and J. Sun, “Delving deep into rectifiers: Surpassing human-level performance on imagenet classification,” in *Proceedings of the IEEE International Conference on Computer Vision*, Dec. 2015, pp. 1026–1034.
- [42] R. K. Srivastava, K. Greff, and J. Schmidhuber, “Training very deep networks,” in *Advances in Neural Information Processing Systems*, vol. 28. Curran Associates, Inc., 2015.
- [43] J. Eccles, “From electrical to chemical transmission in the central nervous system,” *Notes and Records of the Royal Society of London*, vol. 30, no. 2, pp. 219–230, 1976, publisher: The Royal Society. [Online]. Available: <https://www.jstor.org/stable/531754>
- [44] A. Taherkhani, A. Belatreche, Y. Li, G. Cosma, L. P. Maguire, and T. M. McGinnity, “A review of learning in biologically plausible spiking neural networks,” *Neural Networks*, vol. 122, pp. 253–272, Feb. 2020.

A Theoretical Complexity

A.1 Assumptions

The network Consider a fully-connected neural network with K linear layers i computing $h_i = W_i h_{i-1}$. For simplicity, we omit the biases without loss of generality, assume $K > 2$, and furthermore omit non-linear activations, thus considering only linear networks. Let n_i be the width of layer i , i.e., the dimension of h_i ; then W_i has dimensions $n_i \times n_{i-1}$. For the last layer K , this corresponds to the output size C , i.e., $n_K = C$. For multi-class classification, C corresponds to the number of classes. It follows that the feedback weights B_i have dimension $n_i \times C$.

Complexity We measure the computational complexity by counting the number of fused multiply-add (FMA) operations. We assume the use of basic matrix and vector multiplication algorithms with a complexity of ab FMA for both the outer product xy^T and the matrix-vector product Ax with vectors $x \in \mathbb{R}^b$, $y \in \mathbb{R}^a$ and matrix $A \in \mathbb{R}^{a \times b}$.

Memory We measure memory by multiplying the number of elements with the size of their data type. We assume floating point values are stored with 32-bit precision, the default precision in PyTorch [40].

The training For simplicity, we use a batch size of one and assume a basic weight update $W_i \leftarrow W_i - \eta \delta W_i$ with a scalar learning rate $\eta > 0$.

A.2 Complexity of Backpropagation and F³

Forward pass In layer i , the forward pass computes $h_i = W_i h_{i-1}$, which is a matrix-vector multiplication with dimensions $n_i \times n_{i-1}$ and n_{i-1} , thus requiring $n_{i-1} n_i$ FMA. For the whole network, this results in

$$\sum_{i=1}^K n_{i-1} n_i \text{ FMA} \quad (14)$$

Backward pass The backward pass in layer $i \in [1, K-1]$ consists of computing the gradient δh_i using either backpropagation or F³, followed by computing δW_i based on δh_i . With backpropagation, $\delta h_i = W_{i+1}^T \delta h_{i+1}$ resulting in $n_i n_{i+1}$ FMA, whereas with F³, $\delta h_i = B_i^T e_{i-1}$ with the delayed error vector e_{i-1} , which has dimension C , resulting in $n_i C$ FMA. For both backpropagation and F³, the weight gradient is computed with the outer product $\delta W_i = \delta h_i h_{i-1}^T$ requiring $n_{i-1} n_i$ FMA. For the whole network, this results in

$$\underbrace{\sum_{i=2}^K n_{i-1} n_i}_{\text{for } \delta h_i} + \underbrace{\sum_{i=1}^K n_{i-1} n_i}_{\text{for } \delta W_i} \text{ FMA} \quad (15)$$

when using backpropagation and

$$\underbrace{C \sum_{i=1}^{K-1} n_i}_{\text{for } \delta h_i} + \underbrace{\sum_{i=1}^K n_{i-1} n_i}_{\text{for } \delta W_i} \text{ FMA} \quad (16)$$

when using F³.

Update step The weights are updated with $W_i \leftarrow W_i - \eta \delta W_i$, which has complexity $n_{i-1} n_i$ FMA as it requires one FMA per entry of W_i . Updating all layers thus requires

$$\sum_{i=1}^K n_{i-1} n_i \text{ FMA} . \quad (17)$$

Total complexity to process a sample With backpropagation, the total complexity to process one training sample is

$$\underbrace{\sum_{i=1}^K n_{i-1} n_i}_{\text{forward pass}} + \underbrace{\sum_{i=2}^K n_{i-1} n_i}_{\text{backward pass}} + \underbrace{\sum_{i=1}^K n_{i-1} n_i}_{\text{update}} \text{ FMA} = 3 \sum_{i=1}^K n_{i-1} n_i + \sum_{i=2}^K n_{i-1} n_i \text{ FMA}, \quad (18)$$

while with F^3 it is

$$\underbrace{\sum_{i=1}^K n_{i-1} n_i}_{\text{forward pass}} + \underbrace{C \sum_{i=1}^{K-1} n_i}_{\text{backward pass}} + \underbrace{\sum_{i=1}^K n_{i-1} n_i}_{\text{update}} \text{ FMA} = 3 \sum_{i=1}^K n_{i-1} n_i + C \sum_{i=1}^{K-1} n_i \text{ FMA}. \quad (19)$$

A.3 Gain From Using F^3 in Equal-Width Networks

Assuming all hidden layers $i \in [1, K-1]$ have the same width $n_i = w$, the complexity of processing one training sample corresponds to

$$3(n_0 w + \sum_{i=2}^{K-1} w^2 + wC) + \sum_{i=2}^{K-1} w^2 + Cw \text{ FMA} = 3w(n_0 + (K-2)w + C) + (K-2)w^2 + Cw \text{ FMA}, \quad (20)$$

while with F^3 it is

$$3(n_0 w + \sum_{i=2}^{K-1} w^2 + wC) + C \sum_{i=1}^{K-1} w \text{ FMA} = 3w(n_0 + (K-2)w + C) + C(K-1)w \text{ FMA}. \quad (21)$$

Using F^3 over backpropagation thus reduces the complexity by

$$(K-2)w^2 + Cw - C(K-1)w = (K-2)w(w-C). \quad (22)$$

The relative gain of using F^3 is

$$1 - \frac{C(K-1)w}{(K-2)w^2 + Cw} = \frac{w-C}{w + \frac{C}{K-2}} \quad (23)$$

for computing the gradients δy_i and

$$1 - \frac{3w(n_0 + (K-2)w + C) + C(K-1)w}{3w(n_0 + (K-2)w + C) + (K-2)w^2 + Cw} = \frac{(K-2)(w-C)}{4C + 4Kw + 3n_0 - 8w} \quad (24)$$

in total for the forward, backward, and update pass.

F^3 thus reduces the number of required FMA operations as long as $w > C$, which is the case for most applications. The amount of saved operations increases the deeper and wider the network, that is, the larger K and w . If the width is large enough, F^3 saves nearly 100% of the computation required to compute the δy_i since

$$\lim_{w \rightarrow \infty} \frac{w-C}{w + \frac{C}{K-2}} = 1 \quad (25)$$

and up to 25% of the total computation since

$$\lim_{w \rightarrow \infty} \frac{(K-2)(w-C)}{4C + 4Kw + 3n_0 - 8w} = \frac{1}{4}. \quad (26)$$

For example, in a five layer network with input size $n_0 = 100$, output size $C = 10$, and hidden layer width $w = 200$, F^3 can save more than 90% of operations from computing the δy_i and more than 20% of operations in total throughout the whole batch. With a width of $w = 1024$, this increases to over 98% and 24%, respectively. In practice, implementing this linear network manually, we observe a runtime reduction of 50% for computing the δy_i and 16% over the whole batch.

A.4 Memory Requirements of Backpropagation and F^3

For simplicity, we focus on the difference between backpropagation and F^3 when processing a batch of size b and which information needs to be retained between processing different layers. Hence we do not regard data required by both algorithms, such as the (forward) network weights W_i , optimizer parameters, or temporary intermediate results.

Backpropagation To compute the gradients δW_i in the backward pass, backpropagation needs to store a layer's output h_i from computing it in the forward step of layer i until computing the gradient δW_{i+1} in the backward step of layer $i+1$. While processing the last layer, backpropagation is thus storing the outputs of all previous layers for all batches, which results in

$$\sum_{i=1}^{K-1} n_i b \quad (27)$$

elements.

F^3 Unlike backpropagation, F^3 does not need to remember intermediate results h_i for subsequent gradient computation as it computes gradients and updates weights immediately during the forward step. It does, however, come with the additional cost of storing the feedback weights B_i and the delayed error information e_{t-1} . The feedback weights contain

$$\sum_{i=1}^{K-1} n_i C \quad (28)$$

elements, while the delayed error information e_{t-1} contains C entries for each sample, resulting in

$$C \cdot \# \text{ samples} \quad (29)$$

elements.

Gain From Using F^3 in Equal-Width Networks When storing all elements as 32-bit floating point numbers, F^3 introduces an overhead of

$$\left(\sum_{i=1}^{K-1} n_i C + C \cdot \# \text{ samples} \right) 32 \text{ bit} = 4C \left(\sum_{i=1}^{K-1} n_i + 4C \cdot \# \text{ samples} \right) \text{B} \quad (30)$$

while saving

$$\sum_{i=1}^{K-1} n_i b \cdot 32 \text{ bit} = 4b \sum_{i=1}^{K-1} n_i \text{B}. \quad (31)$$

F^3 can thus reduce the required memory if the overhead introduced by the feedback weights B_i and error information e_{t-1} does not exceed the memory saved from not having to store the intermediate results of the forward pass. In summary, F^3 reduces the total amount of required memory by

$$4b \sum_{i=1}^{K-1} n_i - 4C \left(\sum_{i=1}^{K-1} n_i + \# \text{ samples} \right) \text{B} = 4 \cdot \left((b - C) \sum_{i=1}^{K-1} n_i - C \cdot \# \text{ samples} \right) \text{B}. \quad (32)$$

For example, using the same five layer network with hidden layer width $w = 200$ and output size $C = 10$ from Appendix A.3 and training it on 10 000 training samples with batch size $b = 200$, F^3 saves

$$4 \cdot \left((b - C) \cdot \sum_{i=1}^{K-1} n_i - C \cdot \# \text{ samples} \right) \text{B} = 4 \cdot \left((200 - 10) \cdot \sum_{i=1}^5 200 - 10 \cdot 10000 \right) \text{B} = 208 \text{ kB}. \quad (33)$$

compared to backpropagation. Increasing the width to $w = 1024$ increases the memory saved by F^3 to 2.71 MB.

Further optimizations and general neural networks As shown in Section 4, feedback weights initialized with a trinomial distribution perform as well or better than a Kaiming-He distribution. It is thus not necessary to store the feedback weights as floating point values. A more efficient

encoding of the three possible values $\{-1, 0, 1\}$ would require only 2 bit per element, reducing the total memory for the feedback weights to

$$\sum_{i=1}^{K-1} n_i C \cdot 2 \text{ bit} = \frac{1}{4} C \sum_{i=1}^{K-1} n_i B, \quad (34)$$

reducing the required memory to store the feedback weights by a factor of 16.

Since the feedback weights B_i are fixed throughout the training and are initialized with a random initialization, they can be regenerated by repeating the initialization with the same random state. This reduces the required memory to storing the random state, trading memory consumption for additional compute. Depending on the underlying hardware, one could also utilize read-only memory regions to store the B_i as they are constant, which are often separate from the general, writable memory. Storing B_i in the read-only memory can thus free up space in the writable memory for network parameters and intermediate results.

Finally, most neural networks do not consist of linear layers, and most layers contain at least an activation function and potentially further operations like pooling or normalization. This acts in F^3 's favor since it increases the number of intermediate results backpropagation needs to store for the backward pass, while F^3 is unaffected. Similarly, convolutional layers can increase the amount of memory necessary to store the intermediate results since the weight sharing makes the size of the activation map independent of the weights.

B Hyperparameters and Experimental Results

Table 1: Batch size and maximum number of epochs for different datasets.

	EPOCHS	BATCH-SIZE
MNIST	100	50
CIFAR-10	200	100
CENSUS INCOME	100	100
SGEMM	200	512

Table 2: Learning rate to train a fully-connected network with one hidden layer consisting of 500 neurons on different datasets using either backpropagation (and LLO) or biologically plausible training algorithms (F^3 , DRTP, DFA).

	BP	BIO-PLAUSIBLE
MNIST	10^{-3}	10^{-3}
CIFAR-10	10^{-4}	10^{-3}
CENSUS INCOME	10^{-4}	10^{-4}
SGEMM	10^{-2}	10^{-4}

Table 3: Learning rate to train fully-connected networks of varying depths on the SGEMM dataset using either backpropagation (and LLO) or biologically plausible training algorithms (F^3 , DRTP, DFA).

DEPTH	BP	BIO-PLAUSIBLE
1	10^{-2}	10^{-4}
5	10^{-3}	10^{-5}
≥ 10	10^{-4}	10^{-5}

Table 4: Best test loss achieved throughout the training of a fully-connected network with one hidden layer consisting of 500 neurons on different datasets and with different training algorithms. Mean and standard deviation over ten different random seeds. The classification tasks MNIST, CIFAR-10, and Census Income use BCE loss, while the regression task SGEMM uses MSE loss.

	BP	DFA	DRTP	F^3 -ERROR	F^3 -LOSS	LLO
MNIST	0.14 ± 0.00	0.16 ± 0.01	0.29 ± 0.01	0.23 ± 0.01	0.28 ± 0.01	0.51 ± 0.01
CIFAR-10	2.29 ± 0.01	2.53 ± 0.01	2.42 ± 0.01	2.43 ± 0.01	2.50 ± 0.01	2.63 ± 0.00
CENSUS INCOME	0.99 ± 0.00	0.99 ± 0.00	0.99 ± 0.01	1.00 ± 0.00	0.99 ± 0.00	0.99 ± 0.01
SGEMM	0.00 ± 0.00	0.00 ± 0.00	0.36 ± 0.01	0.01 ± 0.00	0.01 ± 0.00	0.26 ± 0.02

Table 5: Best test accuracy [%] achieved throughout the training of a fully-connected network with one hidden layer consisting of 500 neurons on different datasets and with different training algorithms. Mean and standard deviation over ten different random seeds. Since SGEMM is a regression task, it is not included here.

	BP	DFA	DRTP	F^3 -ERROR	F^3 -LOSS	LLO
MNIST	98.29 ± 0.07	98.08 ± 0.05	95.77 ± 0.13	97.16 ± 0.10	96.23 ± 0.08	93.51 ± 0.18
CIFAR-10	51.23 ± 0.20	44.45 ± 0.18	45.61 ± 0.17	46.04 ± 0.18	44.23 ± 0.25	41.21 ± 0.31
CENSUS INCOME	79.64 ± 0.09	79.61 ± 0.04	79.56 ± 0.11	79.51 ± 0.15	79.56 ± 0.13	79.58 ± 0.09

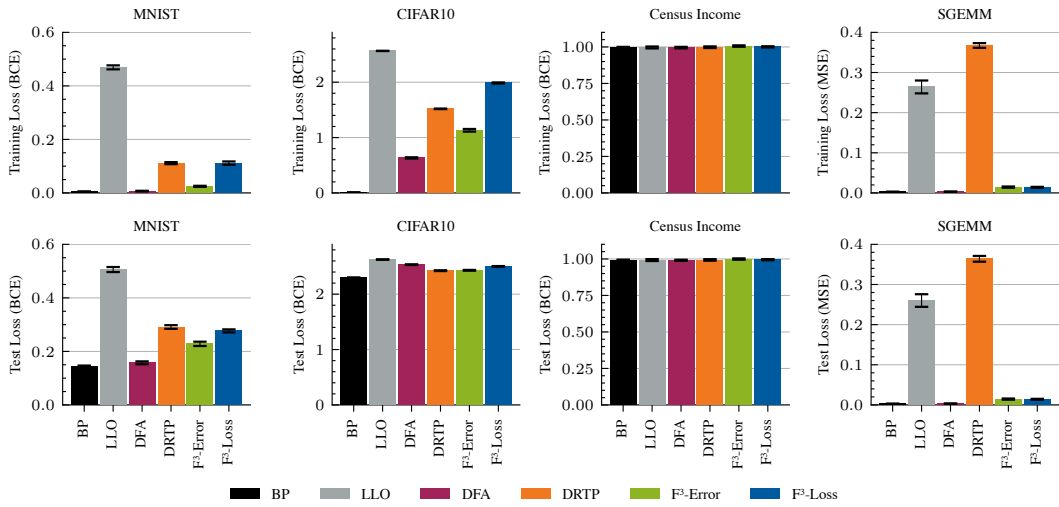


Figure 7: Best loss achieved throughout the training of a fully-connected network with one hidden layer consisting of 500 neurons on different datasets and with different training algorithms. Mean and standard deviation over ten different random seeds.

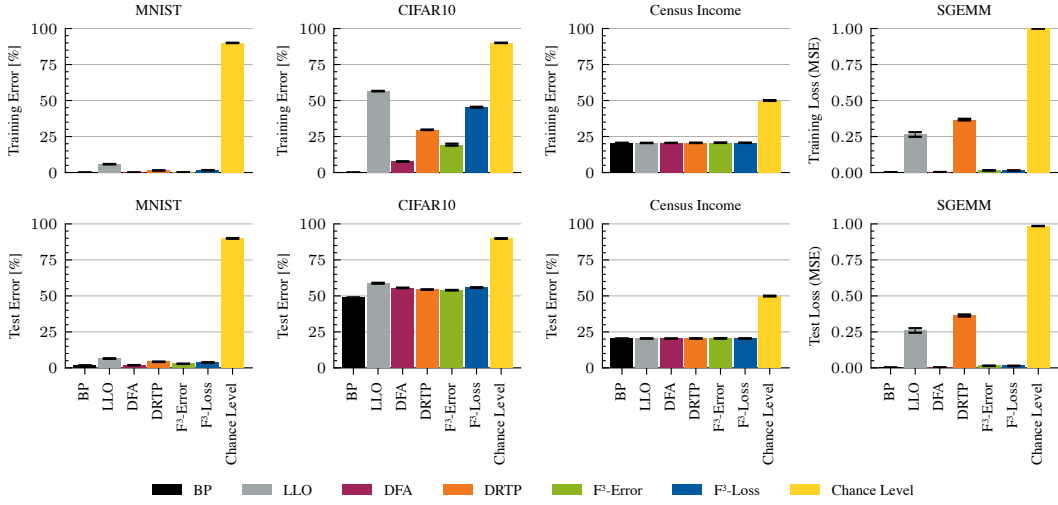


Figure 8: Best error achieved throughout the training of a fully-connected network with one hidden layer consisting of 500 neurons on different datasets and with different training algorithms compared to the chance level (random class weighted by class balance for classification, mean for regression). Mean and standard deviation over ten different random seeds. Since SGEMM is a regression task, the MSE loss is given instead of the top-1-error.

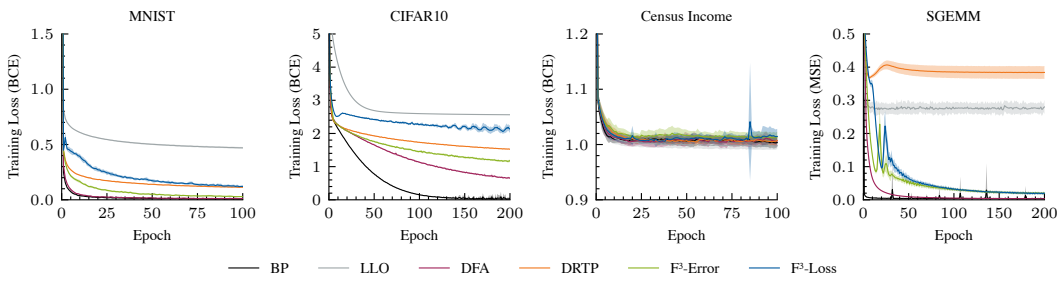


Figure 9: Training loss throughout the training for a fully-connected network with one hidden layer consisting of 500 neurons on different datasets and with different training algorithms. Mean and standard deviation over ten different random seeds.